SERS-based Quantification of PSMA in Tissue Microarrays Allows Effective Stratification of Prostate Cancer Patients

ACS OMEGA

Article

Cite This: ACS Omega 2018, 3, 16784−16794

http://pubs.acs.org/journal/acsodf

SERS-Based Quantification of PSMA in Tissue Microarrays Allows Effective Stratification of Patients with Prostate Cancer

Manjari Bhamidipati,[†] Geuntaek Lee,[‡] Isaac Kim,[‡] and Laura Fabris*[,§]

[†]Department of Biomedical Engineering, Rutgers University, 599 Taylor Road, Piscataway New Jersey 08854, United States

[‡]Cancer Institute of New Jersey-Urology Oncology, Rutgers University, 120 Albany Street, New Brunswick, New Jersey 08901, United States

[§]Department of Materials Science and Engineering, Rutgers University, 607 Taylor Road, Piscataway, New Jersey 08854, United States

Supporting Information

ABSTRACT: Prostate specific membrane antigen (PSMA), a type II membrane protein, is an attractive biomarker that has been validated clinically for the diagnosis of prostate cancer. In this study, we developed surface-enhanced Raman scattering (SERS) nanoprobes for PSMA detection and quantification at the single-cell level on prostate cancer cells. The cells were targeted employing SERS nanoprobes that consisted of gold nanostars functionalized with PSMA aptamer molecules. We were able to quantify picomolar concentrations of soluble PSMA protein and used the resulting calibration curve to estimate the expression of PSMA on the surface of the prostate cancer cell, LNCaP, at the single-cell level. Importantly, we employed these SERS tags to stratify prostate cancer patients by assessing PSMA expression in tissues contained in a prostate tissue microarray. The stratification results clearly correlated PSMA expression to recommended therapy groups, rendering the described method as an effective tool to aid in designing personalized therapeutic protocols. Benchmarking detection sensitivity against immunofluorescence staining and comparing stratification results obtained with the two methods allowed us to validate our novel approach against standard practices. On the basis of these results, we confirm the validity of PSMA as an effective biomarker for prostate cancer patient evaluation and propose SERS-based diagnostic techniques as integrative methods for the assessment of disease stage and the identification of effective therapeutic protocols.

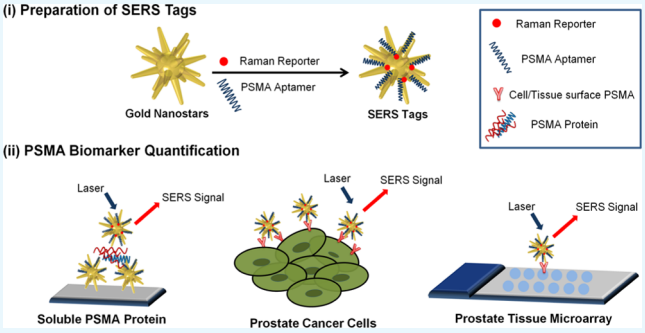

INTRODUCTION

Prostate cancer (PCa) is one of the leading causes of death among male cancer patients.[1] Although often being characterized by slow progression, in some patients it is very aggressive and moves fast from the prostate to the lymph nodes and other distant secondary sites, such as bone. PCa is also characterized as a very heterogenous tissue, which makes accurate diagnosis extremely complex. Current diagnostic practices for prostate cancer assessment include clinical staging, prostate specific antigen (PSA) quantification, and Gleason grading of biopsied tissues. Although these concurrent approaches have been validated and approved, they are still controversial. For instance, PSA levels can increase even in the absence of cancer, as a consequence of other diseases of the prostate, and can be high even after therapy (e.g., androgen deprivation therapy, ADT) as the result of what is known as biochemical recurrence. Therefore, PSA testing can lead to overtreatment. Additionally, Gleason grading, although providing improved matching to clinical outcomes after being revisited in 2014, can still lead to erroneous diagnoses because of the heterogeneity of the tissues and interobserver irreproducibility.[2]

The 2014 revised Gleason grading system assigns a Gleason score to biopsied tissues collected from different sites of the prostate, depending on histological tumor morphology variants, with higher scores assigned to more undifferentiated tissues, i.e., tissues that progressively look less and less like healthy tissues.[3] To make up for the heterogeneity of PCa tissues, the method assigns two scores (e.g., 3 and 4) where the first score is indicative of the structure of the majority tissue (in this case 3), whereas the second describes the minority, surrounding tissue (in this case 4). For this hypothetical sample, the score would then be 3 + 4 = 7. The grading system then compounds the collected scores into grade groups I to V, where I and II are groups for which therapy deferral (or watchful waiting) is recommended, whereas groups III and higher indicate a more advanced disease for which surgery and/or therapy (radiation, hormonal, or chemo) are recommended (see Table 1). The main issue with the Gleason grading system is that it often fails to discriminate among low-

Received: July 31, 2018
Accepted: November 7, 2018
Published: December 6, 2018

DOI: 10.1021/acsomega.8b01839
ACS Omega 2018, 3, 16784−16794

Table 1. Explanation of the Gleason Scoring System[a]

grade group	score 1	score 2	total score
I	≤3	≤3	≤6
II	3	4	7
III	4	3	7
IV	4	4	8
V	4	5	9−10
	5	4	
	5	5	

[a]Score 1 and score 2 are assigned based on histopathology. Higher values for score 1 than score 2 indicate higher disease severity.

risk and high-risk tissues, making it necessary to identify new approaches for patient stratification.[4] One of the recent new approaches for improving diagnosis and patient stratification involves the discovery and use of new biomarkers other than PSA. Among these, the prostate specific membrane antigen (PSMA), a type II transmembrane protein that is specific to all forms of prostate tissue, has been identified as a therapeutically relevant biomarker and validated clinically.[5,6] Increased PSMA expression has been associated with higher recurrence of the tumor,[7] which makes it an attractive target. Although recent literature has shown that PSMA levels accurately correlate with PCa aggressiveness and baseline PSA serum levels, we believe that immunohistochemistry-based assessment can only marginally provide the spatial resolution and sensitivity necessary to take into account the high tissue variability and the PSMA expression level in healthy tissues, calling for the need of a more sensitive and spatially resolved technique. In addition, although antibodies have been used and approved for target recognition in the medical community for quite some time, we believe that substituting them with aptamers for effective target recognition and binding would provide more accurate quantification of PSMA in tissues and therefore more precise stratification of the patients based on their Gleason grade groups.

On the basis of our previous results,[8] we hypothesized that surface-enhanced Raman scattering (SERS) could provide the necessary sensitivity and spatial resolution to enable accurate, tissue-specific correlation of PSMA expression in biopsied specimen of prostate cancer in tissue microarrays (TMAs). SERS-based techniques, employing gold nanoparticles of different sizes and shapes with tunable optical properties, have been used extensively for diagnostic applications.[9,10] They offer excellent biocompatibility and low toxicity and show several advantages over fluorescence, such as the lack of photobleaching. SERS nanoprobes, comprising a plasmonic nanoparticle, a Raman reporter molecule, and targeting molecules (e.g., an aptamer or an antibody), have been shown to effectively target and selectively identify cancerous cells. Among these different components, the shape of the nanoparticle has the most influence on its optical properties and therefore substantially affects the brightness of the nanoprobe.[9] Gold nanostars, in particular, have been shown to possess excellent field enhancement properties, which have enabled single-molecule detection.[11] Furthermore, the use of aptamers, as targeting moieties bound to the nanoparticles, has enabled quantification of biomarker expression in individual PCa cell, making a strong case for the use of these molecules over antibodies.[8]

Herein, we designed and implemented SERS nanoprobes functionalized with PSMA aptamer molecules that allowed us to quantify PSMA expression in prostate cancer cells at the single-cell level and PCa TMAs comprising of biopsied specimens from 34 patients at different stages of the disease. For this purpose, we used a 39-nucleotide PSMA RNA aptamer that was developed by Dassie et al.[12] Extensive characterization of the SERS probes was carried out via transmission electron microscopy (TEM), dynamic light scattering (DLS), ζ potential, and UV−vis spectroscopy. To prove the effectiveness of our SERS probes toward the detection of PSMA, we first built a concentration curve for the SERS-based assay, with which we were able to estimate the expression of PSMA in individual LNCaP prostate cancer cells using aptamers as targeting moieties and PC3 cells as controls, as they are known to not overexpress PSMA. We also compared the effectiveness of aptamers vs antibodies by

Scheme 1. Schematic Overview of PSMA Detection and Quantification Using SERS[a]

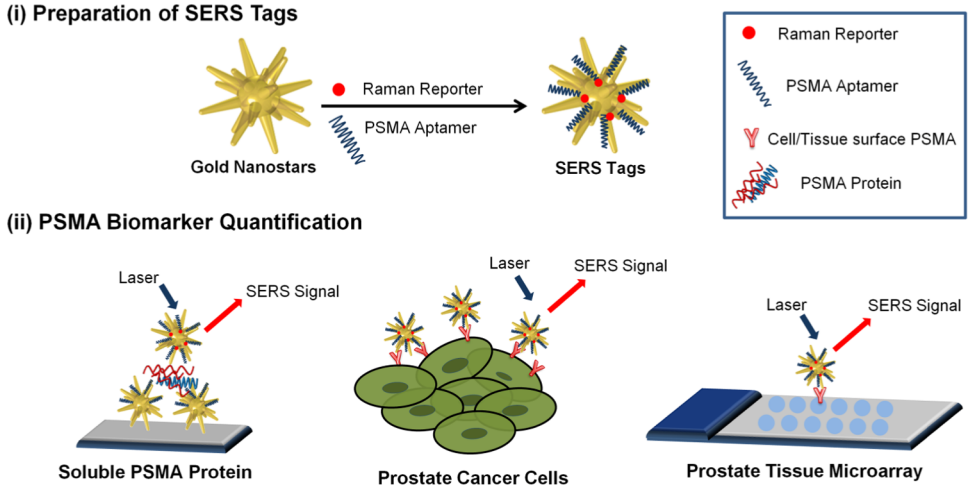

[a]The first step involved synthesis of SERS tags by functionalizing gold nanostars with a thiolated Raman reporter and PSMA aptamer. Following preparation of the SERS tags, a concentration curve was generated using soluble PSMA protein, which was then used to estimate PSMA expression on individual prostate cancer cells, LNCaP. PSMA expression on different tissue specimens contained in a tissue microarray was also detected similarly using SERS tags.

DOI: 10.1021/acsomega.8b01839
ACS Omega 2018, 3, 16784−16794

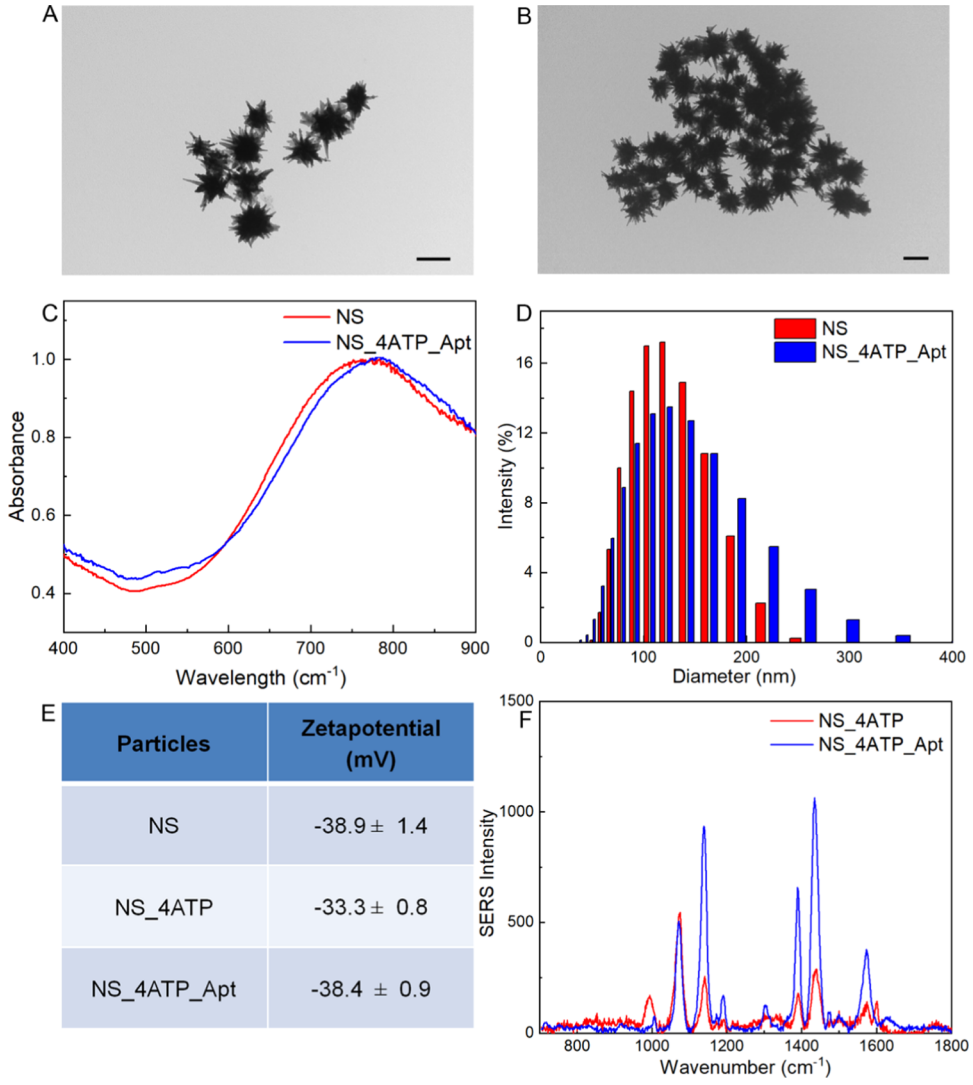

Particles	Zetapotential (mV)
NS	-38.9 ± 1.4
NS_4ATP	-33.3 ± 0.8
NS_4ATP_Apt	-38.4 ± 0.9

Figure 1. Multiple-technique characterization of the synthesized SERS tags. Transmission electron (TEM) micrographs of as-synthesized nanostars (A) and (B) 4-ATP- and PSMA aptamer-functionalized nanostars, respectively. (C) The UV−vis spectra of nanostars before and after functionalization. (D) The dynamic light scattering (DLS) data that show the size distribution of the nanoparticles. (E) The ζ potential (mV) values of the functionalized nanostars with 4-ATP and PSMA aptamer. Mean ± standard deviation values were calculated with $n = 3$ readings for each sample. (F) The SERS spectra of 4-ATP-coated nanostars and nanostars coated with 4-ATP and PSMA aptamer.

targeting PSMA in LNCaP cells using fluorescently labeled aptamers and antibodies, demonstrating a substantially higher recognition with the former. These SERS tags were then used to estimate the expression of PSMA in prostate TMAs, using immunofluorescence staining (IF) as the benchmarking technique in which specimens with Gleason scores between 6 and 9 were present. An overview of the entire procedure for the preparation of SERS tags and PSMA quantification has been shown in Scheme 1. Our results show that SERS outperforms fluorescence-based immunohistochemistry for quantification of PSMA and enables the stratification of patients in three clearly distinct recommended therapy groups, namely, the watchful waiting group (group 1), the non-metastatic active therapy group (group 2), and the metastasized and/or castration resistant group (group 3), based on compounded PSMA expression data. This retrospective study allowed not only to confirm PSMA as an effective biomarker for the evaluation of disease stage but also led to an improved stratification of patients into groups of recommended therapeutic regimen. In the future, the implementation of the approach in longitudinal studies promises to become a valuable method for monitoring disease progression and response to therapy.

RESULTS AND DISCUSSION

Preparation of SERS Tags. The first step in the preparation of SERS nanoprobes was the synthesis of gold nanostars that were synthesized according to a previously reported surfactant-free protocol.[13] The synthesized nanostars had a localized surface plasmon resonance (LSPR) band centered around 773 nm. They were then functionalized with 4-aminothiophenol (4-ATP), the Raman reporter, and the thiolated PSMA aptamer. Functionalization of the reporter and the aptamer to the nanoparticles was enabled by the thiol−Au bond formation. The morphology and size of the nanoparticles before and after functionalization were verified by TEM (Figure 1). TEM micrographs (Figure 1A,B) revealed that the nanostars possess a large number of sharp protruding tips, which were retained upon functionalization with the reporter and the aptamer, thereby ensuring retention of their

DOI: 10.1021/acsomega.8b01839
ACS Omega 2018, 3, 16784−16794

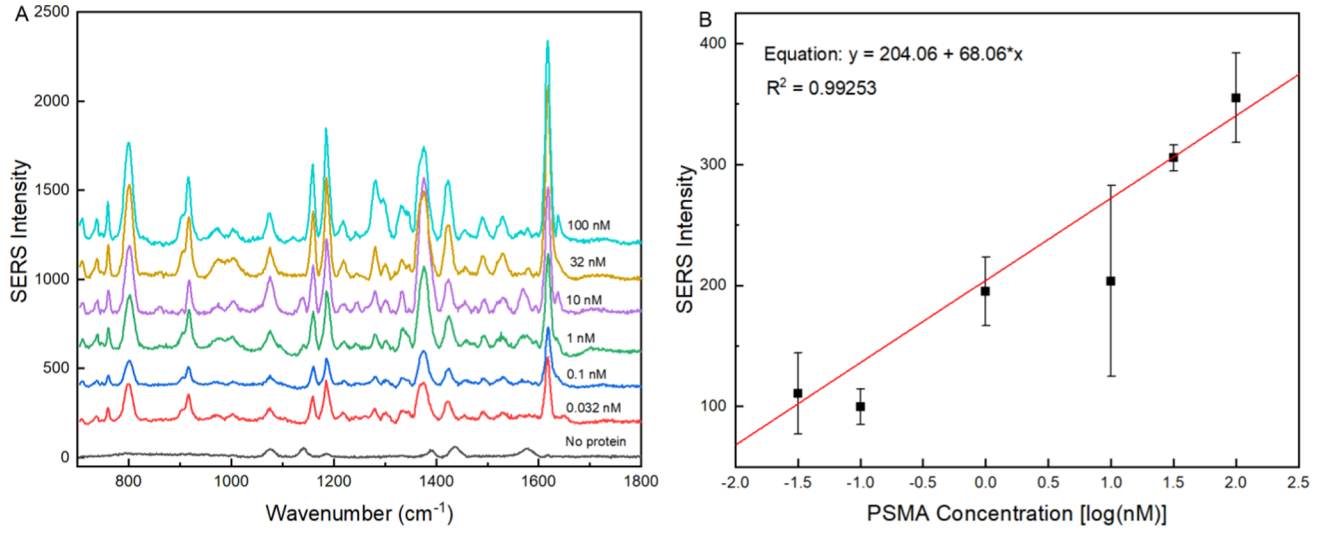

Figure 2. SERS signal dependence on concentration of soluble PSMA protein. (A) The SERS peaks observed between 700 and 1800 cm^{-1} for protein concentrations between 32 pM and 100 nM. A sample lacking the protein was used as a control. A linear dependence between intensity of the 1438 cm^{-1} Raman peak and the log of the PSMA concentration can be appreciated (B).

morphology-dependent SERS activity. The size of the nanoparticles was found to increase by 12 nm from 98.5 ± 15.1 to 110.5 ± 9.1 nm. This increase in size for the nanostars is consistent with the contributions of the added Raman reporter and PSMA aptamer. In addition to this, a slight red shift from 773 to 783 nm in the LSPR position of the nanostars after functionalization was also observed (Figure 1C), which originates as a consequence of its dependence on the dielectric function of the surrounding environment.[14] Dynamic light scattering (DLS) (Figure 1D) further confirmed the increase in the hydrodynamic diameter of nanostars from 120.6 ± 1.8 to 129.6 ± 3.5 nm for nanostars functionalized with both 4-ATP and PSMA aptamer. Upon binding of the SERS tags with protein, the size of the nanostars further increased to 141.2 ± 8.2 nm (Figure S1), confirming retention of PSMA aptamer function after immobilization on the surface of the nanostars.

The functionalization of the nanostars was also confirmed using ζ potential measurements acquired using a Zetasizer. The results of the surface charges of the nanostars are summarized in Figure 1E. We measured a decrease in ζ potential from −38.9 ± 1.4 to −33.3 ± 0.8 mV after addition of 4-ATP to surfactant-free stars, as expected. Upon addition of the negatively charged RNA aptamer, the nanoparticles displayed an increase in the negative charge to −38.4 ± 0.9 mV. These results further confirmed the successful addition of 4-ATP and PSMA aptamer on the nanoparticles.

To quantify the amount of RNA aptamer functionalized on the tags and thus ensure the reproducibility and accuracy of the results, nanostars at different concentrations (1.5 and 3 nM) were loaded with different ratios of the reporter molecules, 4-ATP, and the thiolated PSMA aptamer. The amount of free RNA leftover in the supernatant was then quantified using a Quant-iT OliGreen ssDNA reagent, which is a sensitive fluorescent stain that binds to oligonucleotides in solution. On the basis of the results of this assay (Figure S2), we observed a capture efficiency of 50.02 ± 0.53% when a concentration of 3 nM nanostars was functionalized with 1 μM concentration of 4-ATP and 0.5 μM of PSMA aptamer. These concentrations were found to lead to the highest Raman peak intensity for 4-ATP and were thus chosen for further experiments.

Binding of PSMA aptamer molecules to the nanoparticles was confirmed using SERS measurements. For this, SERS tags consisting of nanostars functionalized with the Raman reporter, 4-ATP, were deposited on a glass slide. SERS measurements (three maps of 5 μm × 5 μm size) were averaged and analyzed. The maps revealed strong Raman peaks of 4-ATP at 994, 1076, 1134, 1387, 1438, 1568, and 1605 cm^{-1} assigned to γCC + γCCC (stretching), νCS (stretching), δCH (bending), δCH + νCC (bending + stretching), νCC + δCH (stretching + bending), νCC (stretching), and δNH (bending) modes, respectively.[15−17] Upon further functionalization of the nanoparticles with the thiolated PSMA aptamer, the peak at 994 cm^{-1} reduced in intensity and shifted by less than 5 cm^{-1}, whereas peaks at 1134, 1387, 1438, and 1575 cm^{-1} increased in intensity. The peak at 1438 cm^{-1}, assigned to the stretching of the C−C bond and bending of the C−H bond in 4-ATP molecules, was chosen to build the calibration curve for soluble PSMA, based on its consistent prominence after aptamer binding.

Correlating SERS Intensity with Protein Concentration. To correlate SERS intensity and PSMA concentration, we captured soluble PSMA at varying concentrations on functionalized glass substrates and measured the resulting SERS response. The first step in the preparation of the protein substrates was the tethering of the gold nanostars (3 nM) to the glass substrate via silanol-based chemistry. The nanostar concentration was chosen since it was previously determined to result in a uniform distribution on the substrate with minimal clustering of particles.[8] We then deposited the 39-nucleotide thiolated PSMA aptamer, A10-3.2, developed by Dassie et al.[12] at a concentration of 1 μM. The thiol group on the aptamer enabled binding of the aptamer to the gold nanostars. Nonspecific binding of the PSMA aptamer on the surface of the gold nanoparticles was avoided via backfilling with 6-mercaptohexanol (MCH).[18] Different concentrations of PSMA protein (32 pM to 100 nM) prepared in Milli-Q water were then deposited on the substrate. Finally, SERS tags were added for identification and localization of PSMA via aptamer targeting. SERS-based quantification of the captured PSMA was then carried out, as reported in Figure 2, in which each

DOI: 10.1021/acsomega.8b01839
ACS Omega 2018, 3, 16784−16794

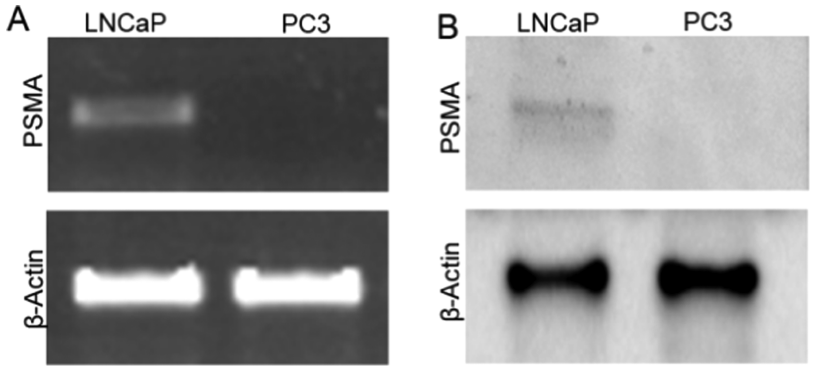

Figure 3. Confirmation of the expression of PSMA in LNCaP cells. (A) The RT-PCR results observed in the prostate cancer cells, LNCaP, and PC3, whereas (B) is the western blot analyses of LNCaP and PC3 cells. Both experiments confirm the expression of PSMA in LNCaP cells, whereas PC3 cells show no expression of PSMA. β-Actin was used as a loading control in both experiments.

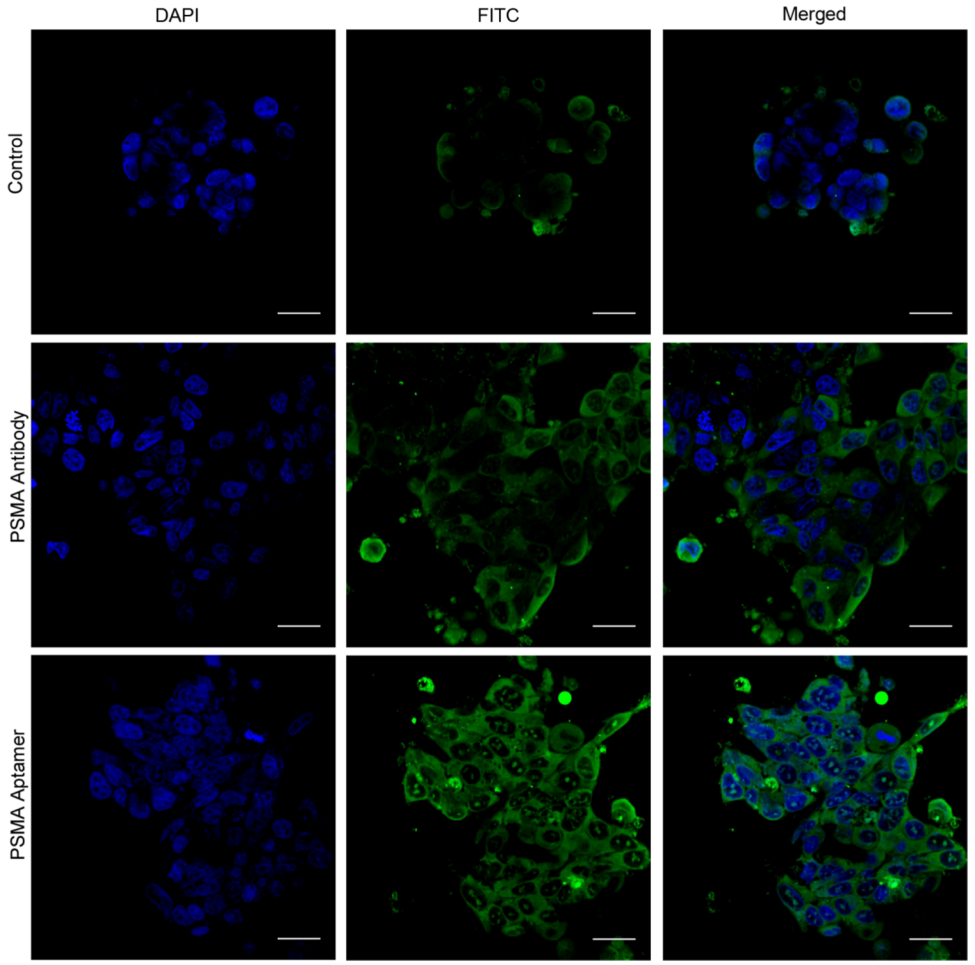

Figure 4. Fluorescent staining of LNCaP cells with PSMA antibody and PSMA aptamer that were conjugated to the fluorophore Alexa Fluor 488. Cell nuclei were stained with 4′,6-diamidino-2-phenylindole (DAPI). Control samples are unstained cells. Scale bars represent 30 μm.

data point was obtained by averaging three 5 μm × 5 μm location agnostic maps on each substrate. A linear dependence between the intensity of 1438 cm^{-1} ATP Raman peak and the PSMA concentration was determined, with a linear correlation (R^2 = 0.99253) between the SERS intensity at 1438 cm^{-1} and the log of protein concentration, between the concentrations of 0.032 and 100 nM. Interestingly, additional peaks were observed when the soluble PSMA protein was deposited on the substrates, which upon further analysis were assigned to both PSMA aptamer and PSMA protein (Figure S3).

Expression of PSMA in Prostate Cancer Cells. Prior to SERS experiments on the prostate cancer cells LNCaP and PC3, the expression of PSMA in these cells was confirmed using reverse transcription polymerase chain reaction (RT-PCR) and western blot analysis. For RT-PCR, both cells were lysed, and the RNA was extracted. A commercially available cDNA reverse transcription kit was then used to convert the RNA to cDNA. The resultant cDNA was employed for quantitative PCR analysis, which showed a high expression of PSMA in LNCaP cells and no expression in PC3 cells, as seen

DOI: 10.1021/acsomega.8b01839
ACS Omega 2018, 3, 16784−16794

in Figure 3A. The results were further confirmed with western blot analysis. For this, the cells were lysed, and their protein content was extracted via sodium dodecyl sulfate-polyacrylamide gel electrophoresis (SDS-PAGE). The protein extracts were then incubated with a primary PSMA antibody and the appropriate secondary antibody. Similar to what we observed with PCR, the results shown in Figure 3B revealed moderate to high expression of PSMA in LNCaP cells and no PSMA expression in PC3 cells. For both experiments, β-actin was used as a loading control.

To test the binding of the PSMA aptamer with LNCaP cells, a thiolated PSMA aptamer conjugated to a fluorophore, Alexa Fluor 488, was used. Both LNCaP and PC3 cells were labeled with the aptamer and imaged. As a comparison, the cells were also stained with a primary PSMA antibody conjugated to Alexa Fluor 488. Results seen in Figure 4 show that both PSMA aptamer and antibody were able to bind to LNCaP cells, with the aptamer showing higher affinity for the LNCaP cells when compared to the antibody. Furthermore, SERS tags conjugated with a Cy3 dye were also added to the LNCaP cells stained with a PSMA antibody conjugated to the Alexa Fluor 488 dye (Figure S4). The images confirmed that the PSMA aptamer-functionalized SERS tags bind to the PSMA expressed on the LNCaP cells. As expected, no fluorescence was observed when PC3 cells were stained with either PSMA aptamer or PSMA antibody (Figure S5).

A cell viability assessment was then carried out to determine the safest concentration of tags that could be loaded in the cell culture while providing a sufficiently intense SERS response. LNCaP cells were incubated with a range of nanoparticle concentrations from 1 to 5 nM for 24 h. The cell viability was then assessed via a 3-(4,5-dimethylthiazol-2-yl)-2,5-diphenyltetrazolium bromide (MTT) proliferation assay. The results were normalized with respect to the untreated control. Figure 5 reveals that the cells remained viable and comparable to the control at all concentrations of nanoparticles. Since analysis of variance (ANOVA) showed no statistical differences between the groups, SERS tags at a concentration of 3 nM were used for PSMA quantification.

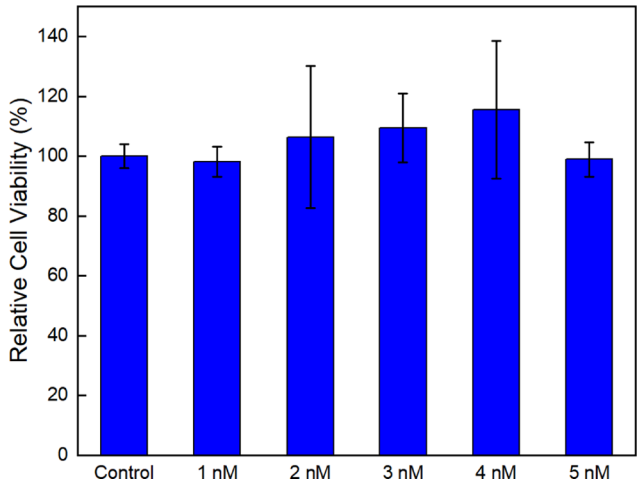

Figure 5. Cell viability results via MTT proliferation assay show the relative cell viability observed in LNCaP cells after exposure to different concentrations of gold nanostars functionalized with 4-ATP and PSMA aptamer for 24 h. Viability results have been normalized to the control (without nanoparticles). Error bars represent standard deviation with $n = 3$.

SERS Analysis of Cells. PSMA expression in LNCaP and PC3 cells was measured at the single-cell level using SERS. Both prostate cancer cells were counted and plated in a tissue culture plate and allowed to attach overnight. They were then incubated with a 3 nM concentration of SERS tags, i.e., gold nanostars functionalized with the Raman reporter, 4-ATP, and PSMA aptamer. The cells were washed thoroughly and fixed before SERS measurements. Three 5 μm × 5 μm maps were acquired for each cell and averaged. Figure 6A shows the SERS spectra obtained from LNCaP cells incubated with the SERS tags. Data acquired from five individual cells showed slight variation in SERS intensity, which could be due to expected differences in marker expression within the same cell population or to differences in nanoparticle uptake. The average SERS spectra from LNCaP cells seen in Figure 6B were considered to be representative of the entire cell population, with an expected range of variability as that observed among the various cells. On the other hand, PC3 cells, known to not overexpress PSMA, were found to possess Raman peaks with very low intensity. Binding of LNCaP cells with a nonspecific aptamer, Mucin-1, also resulted in Raman peaks with very low intensity (Figure S6).[19]

A linear correlation ($R^2 = 0.99242$) was determined between the log of the number of protein molecules present per μm^2 area at different protein concentrations and the SERS peak intensities (Figure 7A), described by equation $y = 68.08x + 14.59$. Using this equation as well as the SERS peak intensity measured for the individual LNCaP and PC3 cells at 1438 cm^{-1}, we estimated the density of PSMA molecules on individual cells (Figure 7B). Although the most intense Raman peaks for the protein curve were observed at 1614 cm^{-1}, this peak was not used to estimate the PSMA expression on the LNCaP cells since the intensity observed for the cells at this peak position was very low (Figure S7). As expected, the expression of PSMA on the LNCaP cells was found to be high, whereas PC3 cells had low or negligible surface expression of PSMA.

Analysis of PSMA Expression in Prostate TMA. Prostate tissue microarrays containing biopsied specimens from patients with different clinical stagings were analyzed by first grouping them according to the new grading system outlined by the International Society of Urological Pathology (ISUP) in 2014.[20] The tissue samples were divided into grade groups I–V: grade group I (Gleason score 6), grade group II (Gleason score 3 + 4 = 7), grade group III (Gleason score 4 + 3 = 7), grade group IV (Gleason score 3 + 5 = 8; 5 + 3 = 8), and grade group V (Gleason score 4 + 5 = 9; 5 + 4 = 9). No samples with Gleason score 10 were present in the TMA. The tissues were then further classified in three groups based on the recommended therapy: (1) watchful waiting (no therapy, group 1), (2) nonmetastatic active therapy (group 2), and (3) metastasized and/or castration resistant therapy (including palliative care, group 3). The first group contained tissue samples having a Gleason score 6, group 2 contained tissues with a Gleason score of 7 (3 + 4 = 7 and 4 + 3 = 7), whereas group 3 consisted of tissues with Gleason scores of 8 and 9.

To compare SERS imaging against immunofluorescence staining for PSMA quantification in TMAs, the prostate TMA samples were first deparaffinized and hydrated. For IF experiments, the tissue sections were stained with a primary PSMA antibody and an appropriate secondary antibody conjugated with TRITC. The cell nuclei were stained with DAPI, and the TMA was imaged. Analysis from IF seen in

DOI: 10.1021/acsomega.8b01839
ACS Omega 2018, 3, 16784–16794

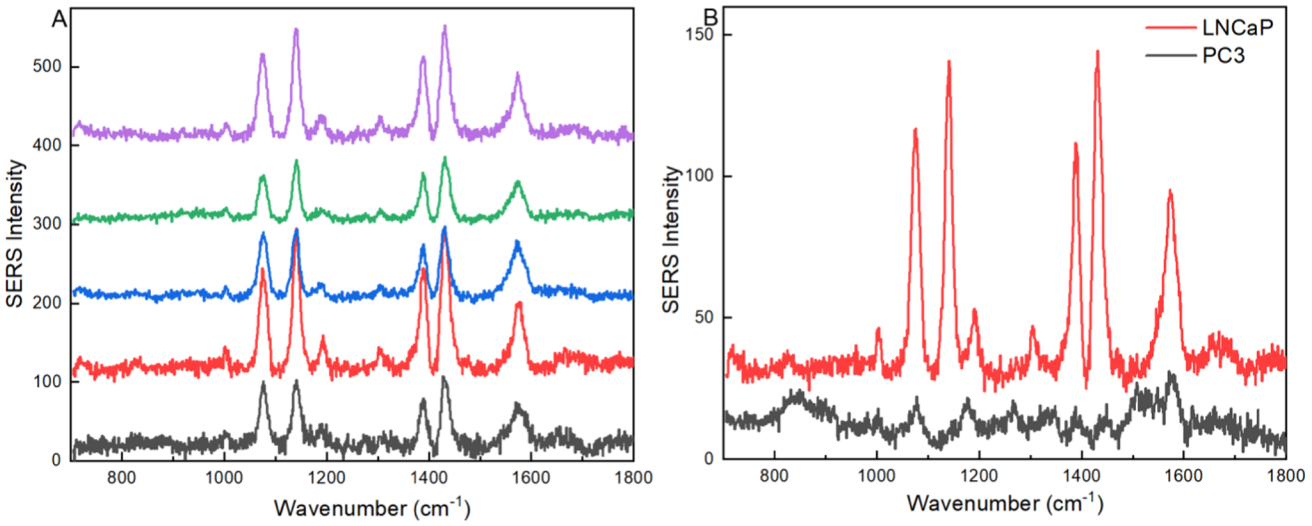

Figure 6. SERS spectra seen in LNCaP cells incubated with nanostars functionalized with 4-ATP and PSMA aptamer. (A) The variation in SERS intensity seen at the single-cell level in five different LNCaP cells. Further assessment of assay selectivity was carried out by incubating PC3 cells that have no surface expression of PSMA. Results from this are shown in (B).

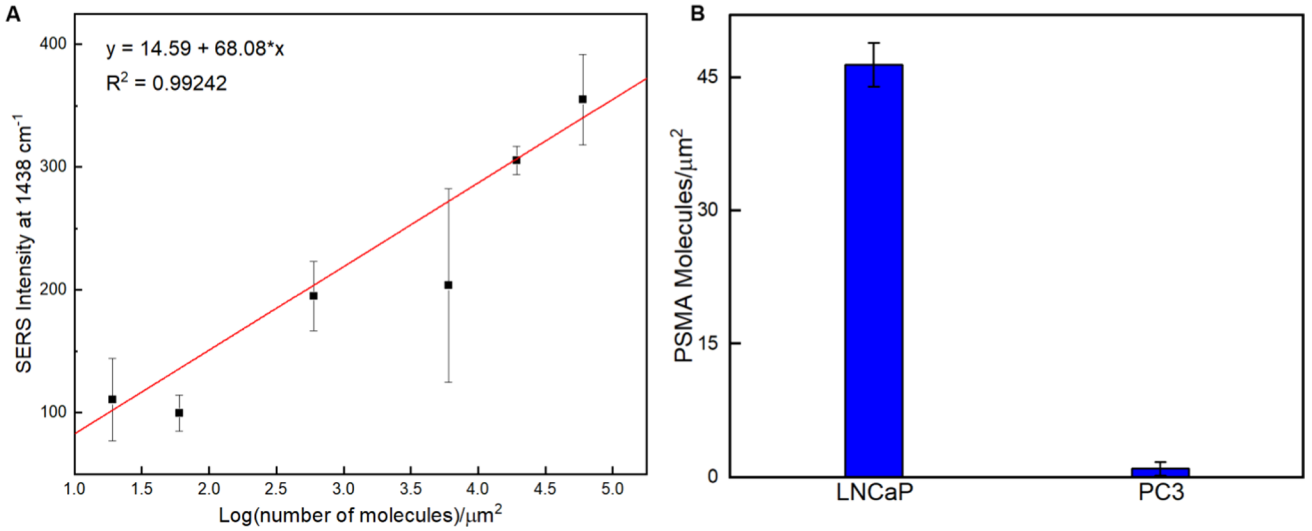

Figure 7. Quantification of PSMA expression seen on individual prostate cancer cells. (A) The linear correlation (R^2 = 0.99242) between log of the number of PSMA molecules found per μm^2 area at different protein concentrations and their SERS response at 1438 cm^{-1}. Using this equation, the number of PSMA molecules present per μm^2 area on the surface of prostate cancer cells was calculated and shown in (B). High expression levels of PSMA were observed in LNCaP cells. Error bars represent standard deviation with n = 3.

Figure 8 showed an increase in the fluorescence intensity between group 1 and group 2, whereas no distinct difference in compounded PSMA expression was observed between group 2 and group 3.

For SERS experiments, after incubating each tissue section with SERS tags, an average of five maps was obtained over an area of 100 μm × 100 μm for each tissue section in the TMA. The averaged SERS signal intensities were then compounded into group 1, group 2, and group 3, as defined above, and reported in Figure 9A. Similar to what was observed in IF staining, the SERS intensity increased as the stage of prostate cancer increased, going from group 1 to group 3. To better understand the differences in detection of PSMA with the two methods, the fluorescence intensity from the IF staining was quantified over the entire area of the tissue and subtracted from the background. The intensity was then averaged with samples in the TMA within the same therapy group. Similarly, for SERS measurements, the intensity of the 1438 cm^{-1} peak was averaged for all samples according to the same classification strategy. A side by side comparison between the intensities revealed a similar pattern, in which substantial increase in PSMA expression levels occurs between the lowest (group 1) and the highest (group 3) groups. However, the analysis of the intermediate group 2 and how it correlates to group 1 and group 3 provide further insight. Two important differences can be gathered from the SERS results: (a) the SERS-based quantification of PSMA allows to differentiate group 1 from group 2 based on the larger spread of the data points in group 2, consistent with the increased tissue heterogeneity that is typical of high Gleason score cancerous tissues and cannot be correlated to variability in enhancement factors of the SERS tags (Supporting Information); (b) a clear differentiation in average PSMA expression levels, in addition to further spreading data points, describes group 3 in line with

DOI: 10.1021/acsomega.8b01839
ACS Omega 2018, 3, 16784−16794

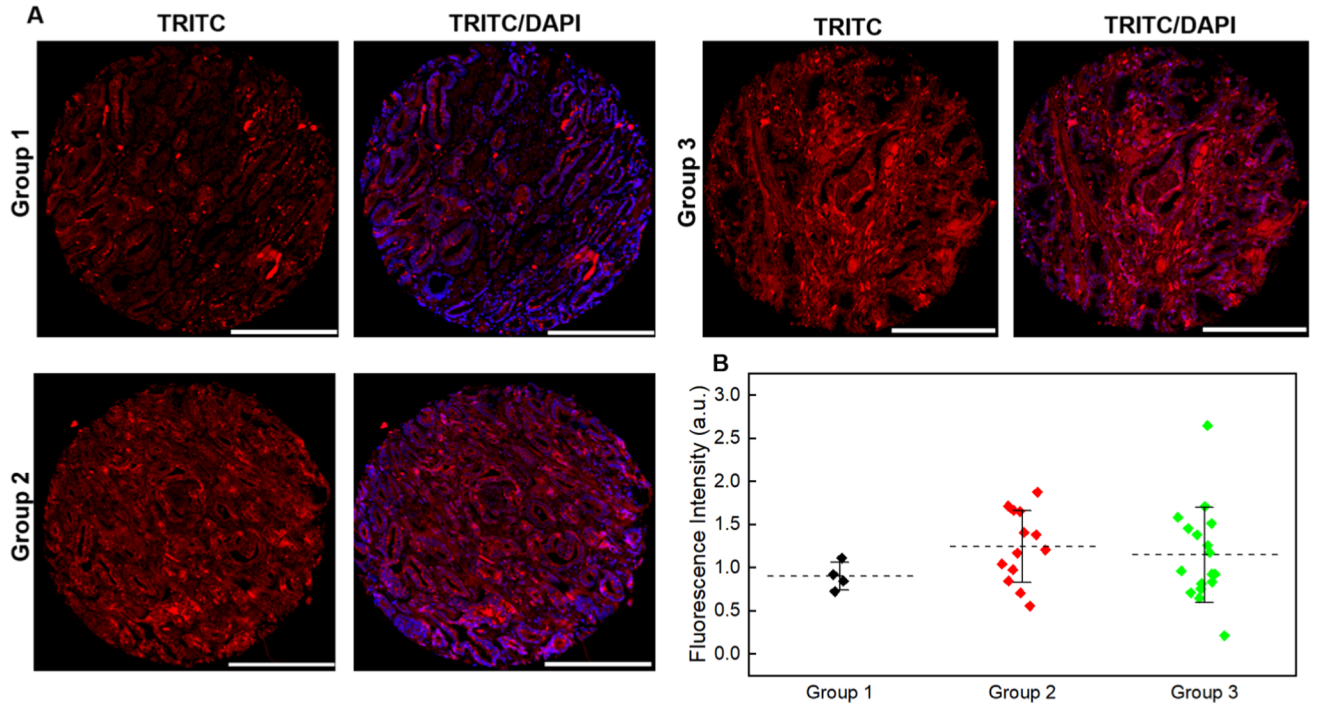

Figure 8. (A) Representative immunofluorescence staining results of a prostate tissue microarray stained with a primary PSMA antibody and a secondary antibody conjugated with TRITC. Cell nuclei have been stained with DAPI. (B) Fluorescence intensity (background subtracted) obtained from immunofluorescence staining of the prostate TMA. The prostate tissue sections have a pathological status ranging from grade groups 1−5 and show increasing PSMA expression in going from group 1 to group 2, whereas no clear differentiation was possible between group 2 and group 3. Scale bars represent 200 μm.

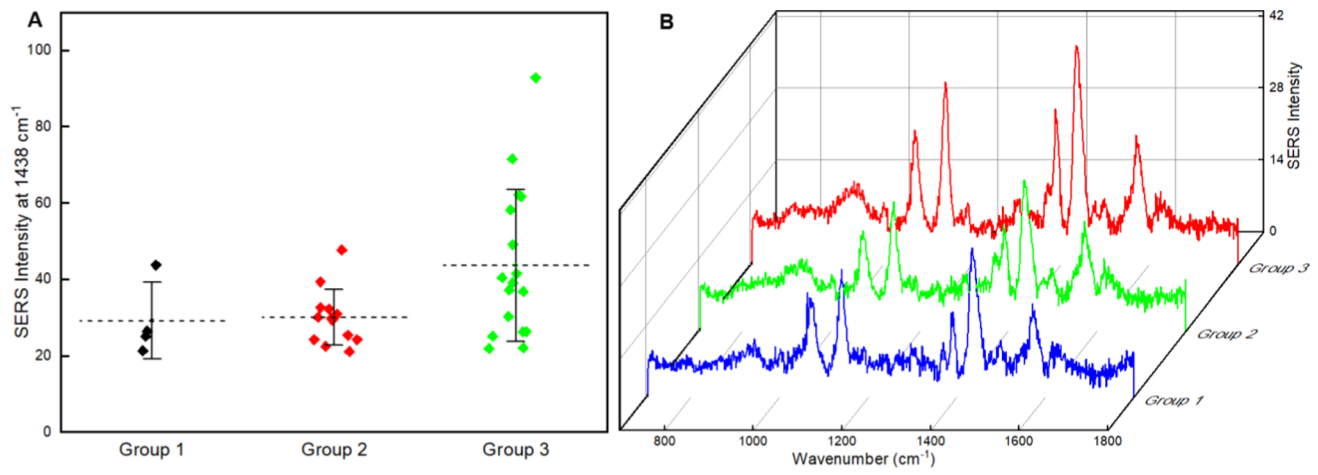

Figure 9. SERS spectra of the prostate tissue microarrays that were incubated with SERS tags. (a) SERS intensity of the 1438 cm^{-1} peak of the spectra obtained from the prostate TMA at different disease stages compounded in groups 1, 2, and 3 depending on recommended therapy. SERS data points become substantially more spread with increasing disease severity, consistent with tissue heterogeneity. (B) Averaged SERS spectra for the three groups show clear increase in the intensity of the 1438 cm^{-1} peak between groups 2 and 3, consistent with higher PSMA expression in advanced stage disease.

tissues with more advanced and/or metastatic character, which are more phenotypically heterogeneous. The clear differentiation in expression levels between groups 1 and 2 and group 3 can be also appreciated looking directly at the SERS data in Figure 9B. Importantly, the spread in PSMA expression levels for various patients classified as high risk and to which aggressive therapy would likely be offered underscores once more the need of detailed biomarker quantification analysis to achieve individualized diagnosis and personalized treatment.

In conclusion, we further demonstrated the validity of PSMA as effective biomarker for stratification of prostate cancer patients, with improved discretization and tissue heterogeneity assessment than possible with fluorescence-based immunohistochemistry. The opportunity of quantifying biomarker expression in tissue microarrays and employing the obtained values as undisputable metrics for therapeutic management promises to aid in the difficult process of staging a patient and providing personalized treatment. By capitalizing from the unsurpassed SERS enhancement properties of gold nanostars and the effective targeting of the PSMA aptamer, we were able to quantify PSMA expression both at the single-cell level and tissue microarrays. Albeit not included in clinical

DOI: 10.1021/acsomega.8b01839
ACS Omega 2018, 3, 16784−16794

trials and only representing a retrospective study of a limited number of prostate cancer patients, our results promise to bring SERS at the forefront among the clinically relevant techniques enabling detailed quantification of biomarker expression. Further implementation of this approach will enable the assessment of other prostate cancer biomarkers and hallmark biomarkers for additional cancer types.

MATERIALS AND METHODS

Nanoparticle Synthesis. Gold nanostars used in the preparation of SERS tags were synthesized according to a previously described protocol developed by Yuan et al.[13] In brief, the synthesis was carried out by combining 2 mL of $HAuCl_4$ salt solution (0.025 M) and 200 μL of 1 N HCl with 48 mL of Milli-Q water. To this mixture, 12 nm citrate-capped spheres (125 μL at A = 2.81) were added and mixed thoroughly by stirring. Finally, 1 mL of ascorbic acid (100 mM) and 2 mL of $AgNO_3$ (3 mM) were simultaneously added. The reaction was stopped after 7 min of stirring. The synthesized surfactant-free nanostars were then purified by centrifugation at 4000g for 10 min.

Preparation of SERS Tags. The thiolated PSMA RNA aptamer A10-3.2 (39 nucleotides) developed by Dassie et al.[12] [5′-HS-$(CH_2)_6$-CAC GGG AGG ACG AUG CGG AUC AGC CAU GUU UAC GUC ACU CCU-3′, Integrated DNA Technologies Inc.] was dissolved in RNAse-free DEPC-treated water (Thermo Fisher). A thiolated Mucin-1 aptamer S2.2 (25 nucleotides)[21] having the sequence [5′-HS-$(CH_2)_6$-GCA GTT GAT CCT TTG GAT ACC CTG G-3′] was used as a negative control for the LNCaP cells. For the fluorescent experiments, the PSMA aptamer was purchased with Alexa Fluor 488 at the 3′ end. For SERS tag synthesis, the gold nanostars were purified and resuspended at a concentration of 3 nM, and then incubated, and allowed to react with 4-aminothiophenol (Sigma-Aldrich) for 30 min at a final concentration of 1 μM. Following this, the thiolated PSMA aptamer was then added to the nanoparticles at a final concentration of 0.5 μM. The prepared SERS tags were allowed to react for an additional 30 min after which they were washed thoroughly and resuspended in Milli-Q water.

Characterization of NPs and SERS Tags. The UV−vis spectra were obtained on an SI Photonics model 440 spectrophotometer. Transmission electron microscopy images of the synthesized nanostars and SERS nanotags were collected on a Philips CM12 transmission electron microscope. On the basis of the TEM images, the size information of the NPs was analyzed using Image J software. Size measurements were also analyzed using DLS measurements. In addition, ζ potential measurements were acquired on a Malvern Zetasizer Nano-ZS instrument. For both DLS and ζ potential measurements, three measurements were performed. For the ζ potential results, the data were fit using Smoluchowski's theory.

The amount of RNA aptamer loaded onto the particles was quantified using Quant-iT OliGreen ssDNA assay kit (Thermo Fisher).

SERS Measurements. The SERS measurements for the protein and cell samples as well as tissue microarrays were carried out using a Renishaw in Via Raman microscope. The spectra were collected using a 633 nm HeNe laser at a laser power of 0.101 mW (20× objective, 1 s acquisition, single accumulation). For all measurements, random areas of the sample were chosen. Maps (5 × 5 μm^2, 3 maps; 1 μm step) were collected for the protein and cell samples, whereas maps of the size 100 × 100 μm^2 (5 maps; 10 μm step) were collected for the tissue microarray samples. The final SERS spectra shown in the results are averages of all of the maps after background subtraction. For internal reference, the intensity of the Si peak at 520 cm^{-1} was used.

Substrate Preparation for Protein Functionalization. The substrates for protein experiments were prepared in a similar way, as described previously.[8] In brief, we used plain glass microscope slides of 0.5 cm × 1 cm size for the protein measurements. The substrates were washed thoroughly and placed in 3-aminopropyltriethoxysilane (APTES) (2% v/v solution) for 20 min after which they were kept in an oven at 110 °C for 1 h. The substrates were backfilled with a 0.3% solution of bovine serum albumin for 1 h. Following this, a suspension of nanostars (3 nM concentration) was incubated on the substrates for 1 h. They were then allowed to bind with PSMA aptamer at 1 μM concentration overnight. The substrates were washed and incubated with 6-mercaptohexanol (MCH) (1 mM) for 1 h. After this, 50 μL of the desired concentration (32 pM to 100 nM concentration) of PSMA protein (Sino Biological Inc.) was deposited on the substrates for 1 h. They were then washed thoroughly and allowed to react with the SERS tags containing PSMA aptamer described above for an additional hour, following which they were analyzed for their SERS activity.

Cell Culture. In this work, PSMA expressing prostate cancer cells, LNCaP, and PSMA-negative cell line, PC3, were used. Both cell lines were grown in RPMI 1640 media (Sigma-Aldrich) that contained 10% fetal bovine serum (Gibco, Thermo Fisher). Cells were grown at 37 °C with 5% CO_2. Expression of PSMA on both cell lines was confirmed by staining the cells with 1:50 diluted PSMA antibody conjugated with Alexa Fluor 488 (Thermo Fisher) and the labeled PSMA aptamer at 2 μM concentration. Cell nuclei were stained with DAPI (Thermo Fisher), as per the manufacturer's instructions. After confirmation of the expression of PSMA on LNCaP cells, the cells were trypsinized and seeded at a density of 20 000 cells/well in a 96-well tissue culture plate. They were allowed to attach for 24 h following which the media was replaced, and SERS tags at a broad concentration range (1−5 nM) were added to the wells. Cell viability was measured using an MTT proliferation assay kit (Thermo Fisher) according to the manufacturer's protocol after exposure to different concentrations of SERS tags for 24 h. For SERS measurements, the appropriate numbers of LNCaP and PC3 cells were counted and plated in a 96-well plate. They were allowed to attach overnight. The medium was then replaced with fresh medium containing SERS nanoprobes at 3 nM concentration. The SERS nanoprobes were allowed to react with the cells for 1 h at 37 °C, following which the cells were washed and fixed with 4% paraformaldehyde in PBS for 10 min. SERS measurements were then carried out on the cells.

Semiquantitative RT-PCR. Total RNA was isolated with TRIzol LS reagent (Thermo Fisher), and 1−2 g of total RNA was used for synthesizing cDNA using a high-capacity cDNA Reverse Transcription Kit (Thermo Fisher). The cDNA was then used for quantitative PCR in a StepOnePlusTM (Applied Biosystems) with SYBR Green ROX qPCR Mastermix (Qiagen) and semiquantitative PCR. The PCR primers for PSMA and β-actin that were used are shown as follows: PSMA (Forward: GAAACCGACTCGGCTGTGG, Reverse: TAAACCACCCGAAGAGGAAGC); β-actin (Forward:

DOI: 10.1021/acsomega.8b01839
ACS Omega 2018, 3, 16784−16794

AGAGCTACGAGCTGCCTGAC, Reverse: AGCACTGTGTTGGCGTACAG).

Western Blot Analysis. Prostate cancer cells (LNCaP and PC3) were collected and lysed with lysis buffer (20 mM Tris-HCl (pH 7.5), 150 mM NaCl, 1 mM Na_2EDTA, 1 mM EGTA, 1% Triton, 2.5 mM sodium pyrophosphate, 1 mM β-glycerophosphate, 1 mM Na_3VO_4, 1 μg/mL leupeptin) along with 1 mM phenylmethylsulfonyl fluoride (PMSF). The cell lysates were centrifuged, and the supernatant was used as protein. After separation of 50 μg of protein via SDS-PAGE, the samples were incubated with a primary monoclonal PSMA antibody (Abcam) and β-actin antibody (Sigma-Aldrich). Following incubation with the appropriate secondary antibody, the immunoblot was analyzed using a SuperSignal West Femto Maximum Sensitivity Substrate (Thermo Fisher).

Tissue Microarray Staining. Paraffin-embedded specimens of 1 mm diameter from 34 prostate cancer patients were mounted on a glass slide as a tissue microarray. All tissue sections had prostatic adenocarcinoma with grade groups 1−5. The pathological status of the tissue samples was: grade group 1 (Gleason score 6) (N = 4), grade group 2 (Gleason score 3 + 4 = 7) (N = 11), grade group 3 (Gleason score 4 + 3 = 7) (N = 3), grade group 4 (Gleason score 3 + 5 = 8; 5 + 3 = 8) (N = 8), and grade group 5 (Gleason score 4 + 5 = 9; 5 + 4 = 9) (N = 8). Removal of paraffin and subsequent rehydration of the tissue sections were carried out by washing the tissue microarray with xylene, ethanol, ethanol/water mixtures, and in distilled water. Antigen retrieval on the tissue sections was carried out by immersing the slide in a pH 6 citrate buffer (10× Citrate Antigen Retrieval Buffer, Sigma-Aldrich) and heating to 95 °C for 20 min. The slide was then cooled to room temperature for 20 min and washed with distilled water. For immunofluorescence staining, the tissue specimens were stained with a primary monoclonal PSMA antibody (Thermo Fisher) followed by a secondary antibody conjugated with TRITC (Thermo Fisher) and imaged. Cell nuclei were stained with DAPI. For SERS measurements, the tissue microarray was incubated with SERS tags at 37 °C for 1 h and then imaged.

Statistical Analyses. Statistical analyses on the samples were performed using a single factor analysis of variance (ANOVA) with a significance value of 0.05 in Origin 9.5 software. The results have been expressed as the average ± standard deviation.

■ ASSOCIATED CONTENT

Supporting Information

The Supporting Information is available free of charge on the ACS Publications website at DOI: 10.1021/acsomega.8b01839.

DLS measurements of SERS tags and SERS tags conjugated with PSMA protein; capture efficiency of PSMA RNA aptamer on the nanoparticles detected using the Quant-iT OliGreen ssDNA kit; SERS peaks of PSMA aptamer and soluble PSMA protein; fluorescent images of LNCaP cells stained with PSMA antibody and SERS tags; fluorescent images of PC3 cells (negative control) stained with PSMA antibody and PSMA aptamer; SERS peaks of LNCaP cells incubated with SERS tags containing a nonspecific aptamer, Mucin-1; SERS intensity peaks observed with different concentrations of PSMA protein at 1438 and 1614 cm^{-1} (PDF)

■ AUTHOR INFORMATION

Corresponding Author

*E-mail: lfabris@soe.rutgers.edu.

ORCID

Laura Fabris: 0000-0002-7089-5175

Notes

The authors declare no competing financial interest.

■ ACKNOWLEDGMENTS

This work was funded through Rutgers Busch Biomedical Grant 17030517.

■ REFERENCES

(1) https://www.cancer.org/cancer/prostate-cancer/about/key-statistics.html.

(2) https://www.cancer.net/cancer-types/prostate-cancer/stages-and-grades.

(3) Shah, R. B.; Zhou, M. Recent advances in prostate cancer pathology: Gleason grading and beyond. *Pathol. Int.* **2016**, *66*, 260−272.

(4) Bravaccini, S.; Puccetti, M.; Bocchini, M.; Ravaioli, S.; Celli, M.; Scarpi, E.; De Giorgi, U.; Tumedei, M. M.; Raulli, G.; Cardinale, L.; Paganelli, G. PSMA expression: a potential ally for the pathologist in prostate cancer diagnosis. *Sci. Rep.* **2018**, *8*, No. 4254.

(5) Ross, J. S.; Sheehan, C. E.; Fisher, H. A.; Kaufman, R. P., Jr.; Kaur, P.; Gray, K.; Webb, I.; Gray, G. S.; Mosher, R.; Kallakury, B. V. Correlation of primary tumor prostate-specific membrane antigen expression with disease recurrence in prostate cancer. *Clin. Cancer Res.* **2003**, *9*, 6357−6362.

(6) Santoni, M.; Scarpelli, M.; Mazzucchelli, R.; Lopez-Beltran, A.; Cheng, L.; Cascinu, S.; Montironi, R. Targeting prostate-specific membrane antigen for personalized therapies in prostate cancer: morphologic and molecular backgrounds and future promises. *J. Biol. Regul. Homeostatic Agents* **2014**, *28*, 555−563.

(7) Minner, S.; Wittmer, C.; Graefen, M.; Salomon, G.; Steuber, T.; Haese, A.; Huland, H.; Bokemeyer, C.; Yekebas, E.; Dierlamm, J.; Balabanov, S.; Kilic, E.; Wilczak, W.; Simon, R.; Sauter, G.; Schlomm, T. High level PSMA expression is associated with early PSA recurrence in surgically treated prostate cancer. *Prostate* **2011**, *71*, 281−288.

(8) Bhamidipati, M.; Cho, H.-Y.; Lee, K.-B.; Fabris, L. SERS-based quantification of biomarker expression at the single cell level enabled by gold nanostars and truncated aptamers. *Bioconjugate Chem.* **2018**, *29*, 2970.

(9) Wang, Y.; Yan, B.; Chen, L. SERS Tags: Novel Optical Nanoprobes for Bioanalysis. *Chem. Rev.* **2013**, *113*, 1391−1428.

(10) Ravanshad, R.; Karimi Zadeh, A.; Amani, A. M.; Mousavi, S. M.; Hashemi, S. A.; Savar Dashtaki, A.; Mirzaei, E.; Zare, B. Application of nanoparticles in cancer detection by Raman scattering based techniques. *Nano Rev. Exp.* **2018**, *9*, No. 1373551.

(11) Rodríguez-Lorenzo, L.; Álvarez-Puebla, R. A.; de Abajo, F. J. G.; Liz-Marzán, L. M. Surface Enhanced Raman Scattering Using Star-Shaped Gold Colloidal Nanoparticles. *J. Phys. Chem. C* **2010**, *114*, 7336−7340.

(12) Dassie, J. P.; Liu, X. Y.; Thomas, G. S.; Whitaker, R. M.; Thiel, K. W.; Stockdale, K. R.; Meyerholz, D. K.; McCaffrey, A. P.; McNamara, J. O., 2nd; Giangrande, P. H. Systemic administration of optimized aptamer-siRNA chimeras promotes regression of PSMA-expressing tumors. *Nat. Biotechnol.* **2009**, *27*, 839−849.

(13) Yuan, H.; Khoury, C. G.; Hwang, H.; Wilson, C. M.; Grant, G. A.; Vo-Dinh, T. Gold nanostars: surfactant-free synthesis, 3D modelling, and two-photon photoluminescence imaging. *Nanotechnology* **2012**, *23*, No. 075102.

(14) Maier, S. A. *Plasmonics: Fundamentals and Applications*; Springer Science & Business Media, 2007.

(15) Hu, X.; Wang, T.; Wang, L.; Dong, S. Surface-Enhanced Raman Scattering of 4-Aminothiophenol Self-Assembled Monolayers in

DOI: 10.1021/acsomega.8b01839
ACS Omega 2018, 3, 16784−16794

Sandwich Structure with Nanoparticle Shape Dependence: Off-Surface Plasmon Resonance Condition. *J. Phys. Chem. C* **2007**, *111*, 6962−6969.
(16) Quynh, L. M.; Nam, N. H.; Kong, K.; Nhung, N. T.; Notingher, I.; Henini, M.; Luong, N. H. Surface-Enhanced Raman Spectroscopy Study of 4-ATP on Gold Nanoparticles for Basal Cell Carcinoma-Fingerprint Detection. *J. Electron. Mater.* **2016**, *45*, 2563−2568.
(17) Osawa, M.; Matsuda, N.; Yoshii, K.; Uchida, I. Charge transfer resonance Raman process in surface-enhanced Raman scattering from p-aminothiophenol adsorbed on silver: Herzberg-Teller contribution. *J. Phys. Chem.* **1994**, *98*, 12702−12707.
(18) Steel, A. B.; Levicky, R. L.; Herne, T. M.; Tarlov, M. J. Immobilization of nucleic acids at solid surfaces: effect of oligonucleotide length on layer assembly. *Biophys. J.* **2000**, *79*, 975−81.
(19) O'Connor, J. C.; Julian, J.; Lim, S. D.; Carson, D. D. MUC1 expression in human prostate cancer cell lines and primary tumors. *Prostate Cancer Prostatic Dis.* **2005**, *8*, 36−44.
(20) Epstein, J. I.; Egevad, L.; Amin, M. B.; Delahunt, B.; Srigley, J. R.; Humphrey, P. A. The 2014 International Society of Urological Pathology (ISUP) Consensus Conference on Gleason Grading of Prostatic Carcinoma: Definition of Grading Patterns and Proposal for a New Grading System. *Am. J. Surg. Pathol.* **2016**, *40*, 244−252.
(21) Ferreira, C. S.; Cheung, M. C.; Missailidis, S.; Bisland, S.; Gariepy, J. Phototoxic aptamers selectively enter and kill epithelial cancer cells. *Nucleic Acids Res.* **2009**, *37*, 866−76.

DOI: 10.1021/acsomega.8b01839
ACS Omega 2018, 3, 16784−16794